

Dependence of the photoluminescence of annealed III-V semiconductor quantum dots on their shape and dimension

Subindu Kumar, Sanjib Kabi, and Dipankar Biswas

Citation: *Journal of Applied Physics* **104**, 086102 (2008); doi: 10.1063/1.2992519

View online: <http://dx.doi.org/10.1063/1.2992519>

View Table of Contents: <http://scitation.aip.org/content/aip/journal/jap/104/8?ver=pdfcov>

Published by the [AIP Publishing](#)

Articles you may be interested in

Presentation and experimental validation of a model for the effect of thermal annealing on the photoluminescence of self-assembled InAs/GaAs quantum dots

J. Appl. Phys. **107**, 123107 (2010); 10.1063/1.3431388

Group-III intermixing in In As/In Ga Al As quantum dots-in-well

Appl. Phys. Lett. **88**, 111110 (2006); 10.1063/1.2181189

Single step quantum well intermixing with multiple band gap control for III-V compound semiconductors

J. Appl. Phys. **96**, 3282 (2004); 10.1063/1.1780608

Anomalous temperature dependence of photoluminescence from InAs quantum dots

J. Appl. Phys. **88**, 2529 (2000); 10.1063/1.1288231

Intermixing induced changes in the radiative emission from III-V quantum dots

Appl. Phys. Lett. **72**, 2850 (1998); 10.1063/1.121478



Dependence of the photoluminescence of annealed III-V semiconductor quantum dots on their shape and dimension

Subindu Kumar,^{a)} Sanjib Kabi, and Dipankar Biswas

Institute of Radiophysics and Electronics, University of Calcutta, 92 A. P. C. Rd., Kolkata 700009, India

(Received 4 June 2008; accepted 20 August 2008; published online 24 October 2008)

Interdiffusion in III-V semiconductor quantum dots (QDs) may occur during growth and subsequent device processing steps. The photoluminescence (PL) spectra of $\text{In}_x\text{Ga}_{1-x}\text{As}/\text{GaAs}$ and $\text{In}_x\text{Ga}_{1-x}\text{N}/\text{GaN}$ QDs change significantly on annealing. The size and shape of a QD dot are important parameters, which govern this change of the PL spectra. In this communication, we have investigated the effects of interdiffusion in realistic $\text{In}_x\text{Ga}_{1-x}\text{As}/\text{GaAs}$ and $\text{In}_x\text{Ga}_{1-x}\text{N}/\text{GaN}$ QDs with various geometries which are of theoretical and practical interest such as pyramidal, truncated pyramidal, and lens shaped, through quantum mechanical computations. © 2008 American Institute of Physics. [DOI: 10.1063/1.2992519]

Photoluminescence¹⁻⁴ (PL) is often used for obtaining informative data from QDs of compound semiconductor interfaces subjected to interdiffusion. There are a number of reports on the annealing of $\text{In}_x\text{Ga}_{1-x}\text{As}/\text{GaAs}$ ^{1,2,4} and $\text{In}_x\text{Ga}_{1-x}\text{GaAs}$ ⁵⁻⁷ QDs. Initially the PL spectrum is broad. After annealing, the PL peaks undergo blueshifts and the full width at half maximum (FWHM) decreases while there is an increase in the intensity. The optical properties of QDs can be improved by tailoring the shape and size of the dots.⁸

The aim of this paper is to investigate the dependence of the PL spectra of annealed $\text{In}_x\text{Ga}_{1-x}\text{As}/\text{GaAs}$ and $\text{In}_x\text{Ga}_{1-x}\text{N}/\text{GaN}$ QDs of various shapes and dimensions. Model quantum mechanical calculations were carried out for pyramidal,^{3,8-10} truncated pyramidal⁸⁻¹⁰ and lens shaped^{8,11} dots. We have stressed on the changes in shapes of the conduction and valence bands and the successive changes in the energy levels due to the variation of the dot shape and size. We have presented the results of such investigations along with necessary comments and discussions.

Typical PL spectra on annealing of $\text{In}_x\text{Ga}_{1-x}\text{As}/\text{GaAs}$ QDs are depicted in Ref. 1. The interpretations of such phenomena that we presented³ are centered around a necessary and important point that when a QD starts growing, a small three dimensional pyramid is formed, which is very rich in indium, as shown in Fig. 1(a).³ As the dot grows in size, the upper layers forming the dot are successively depleted of indium. Thus the conduction band and the valence band of an as grown QD observed from the substrate in the growth direction are asymmetric triangular wells, where there is a continuous variation of both indium and width, as depicted in Fig. 1(b).³ As seen from quantum mechanical computations, large numbers of transition levels are available from the asymmetric triangular wells of widely different depths and widths making the PL spectra of the as grown structure broad. After long annealing, indium outdiffuses from the central core and the indium composition in the dot is homogenized and the asymmetric triangular wells tend toward rectangular, where the variation is in the width only, as illus-

trated in Fig. 1(c).³ The depth becomes constant. The resulting PL arises from the transitions of these wells. Similar interpretations are applicable for In-rich $\text{In}_x\text{Ga}_{1-x}\text{N}/\text{GaN}$ dots and dots having different shapes such as truncated pyramid or lens shaped.

Quantum mechanical computations were carried out for lens shaped, pyramidal and truncated pyramidal $\text{In}_x\text{Ga}_{1-x}\text{As}/\text{GaAs}$, and $\text{In}_x\text{Ga}_{1-x}\text{N}/\text{GaN}$ QD structures. The bases of the pyramidal and truncated pyramidal structures were considered to be square shaped.^{3,9} The variation of indium is assumed to have five concentrations of linear gradient from the central core to the outer periphery,³ with indium varying as $x=0.8, 0.603, 0.405, 0.208, 0.01$ (Ref. 3) or $x=0.6, 0.453, 0.305, 0.158, 0.01$ for two sets of computations

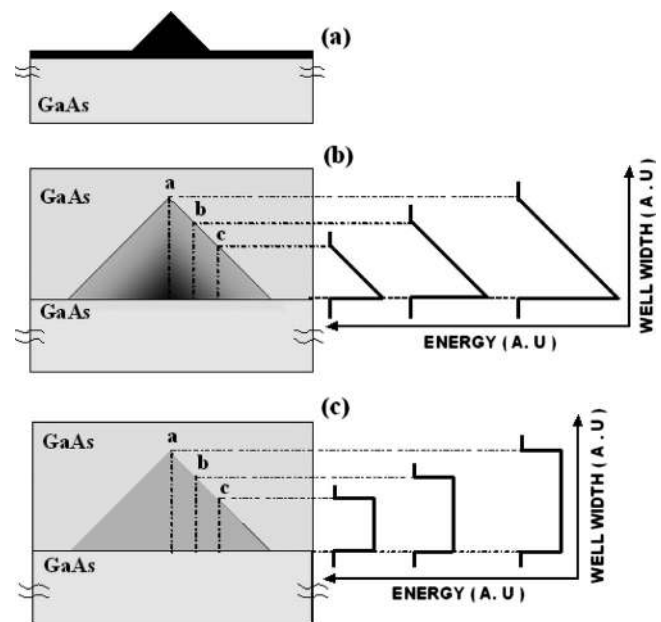


FIG. 1. Schematic illustration of the formation of a QD of $\text{In}_x\text{Ga}_{1-x}\text{As}$ on GaAs. Darker shades indicate higher composition of x . (a) Initial nucleation of indium-enriched island on strained alloy film on substrate. (b) Later stage, when island has consumed alloy film, which becomes progressively indium depleted during growth. (c) Final stage, after annealing, showing the homogenization of indium and gallium. The corresponding conduction bands at different cross sections of the dot are also shown in (b) and (c).

^{a)}Electronic mail: subindukumar@hotmail.com.

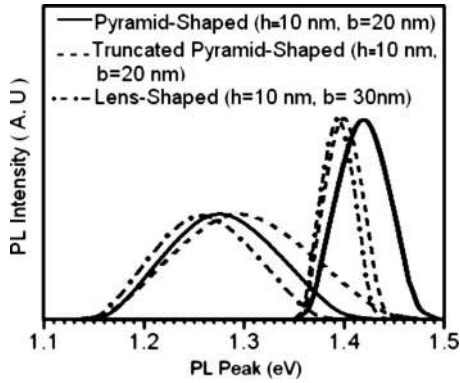


FIG. 2. Schematic representation of the computed PL spectra for triangular and rectangular QWs corresponding to the as grown and of annealed $\text{In}_x\text{Ga}_{1-x}\text{As}/\text{GaAs}$ QDs having pyramidal, truncated pyramidal, and lens shaped geometries.

having initial core concentrations 0.8 and 0.6, respectively, corresponding to both $\text{In}_x\text{Ga}_{1-x}\text{As}/\text{GaAs}$ and $\text{In}_x\text{Ga}_{1-x}\text{N}/\text{GaN}$ QD structures. After annealing, the indium, with no outdiffusion into the barrier, homogenizes throughout the QD to values of $x=0.17$ and $x=0.13$, respectively, for the two sets of computations. The band gap, $E_{g,\text{InGaAs}}$, of $\text{In}_x\text{Ga}_{1-x}\text{As}$ and the energy levels of the finite triangular and the rectangular QWs of different depths and widths were calculated from the formulae outlined in Ref. 3.

In case of $\text{In}_x\text{Ga}_{1-x}\text{As}/\text{GaAs}$ dots, the effective masses³ were obtained through a linear extrapolation between the effective masses of InAs and GaAs. For asymmetric triangular wells the indium concentration was varied from 0.8 to 0.01 and 0.6 to 0.01 for two sets of computations. In case of rectangular well, m_e^* and m_h^* were considered to be $0.060m_0$ and $0.442m_0$, and $0.062m_0$ and $0.444m_0$ for two homogenized indium concentrations, 0.17 and 0.13, respectively. The band offset ratio, $\Delta E_C:\Delta E_V$ for both sets was considered to be 60:40. At the crossovers of the indium concentrations, computations for both the concentrations were done.³ Computations at the same sections of the rectangular wells were also carried out.

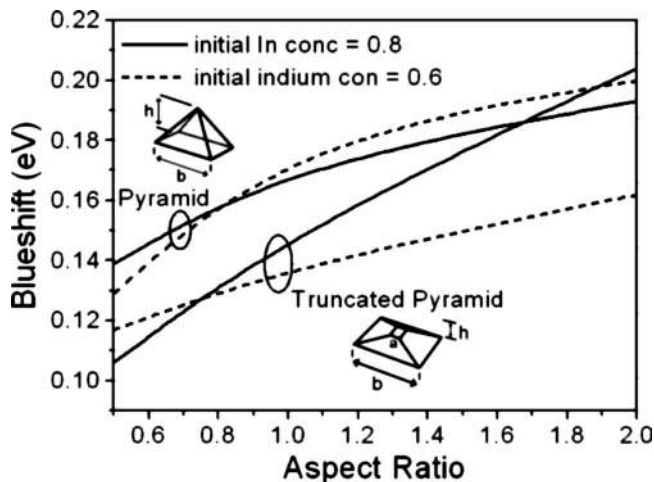


FIG. 3. Variation of the blueshift with the aspect ratio for pyramidal and truncated pyramidal $\text{In}_x\text{Ga}_{1-x}\text{As}/\text{GaAs}$ QDs for two different initial indium concentrations 0.8 and 0.6.

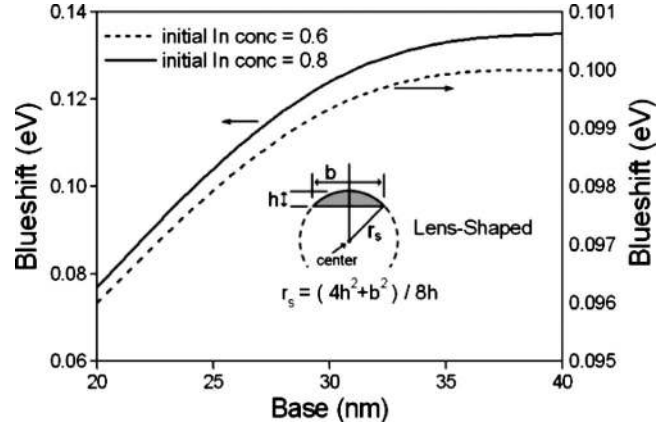


FIG. 4. Variation of the blueshift with the base for lens shaped $\text{In}_x\text{Ga}_{1-x}\text{As}/\text{GaAs}$ dots for two different initial indium concentrations 0.8 and 0.6.

Similar computations were carried out for $\text{In}_x\text{Ga}_{1-x}\text{N}/\text{GaN}$ QD structures. The band gap, $E_{g,\text{InGaAs}}$, of $\text{In}_x\text{Ga}_{1-x}\text{N}$ is determined from the empirical relation¹²

$$E_{g,\text{InGaAs}} = xE_{g,\text{InN}} + (1-x)E_{g,\text{GaAs}} - bx(1-x), \quad (1)$$

where $E_{g,\text{InN}}$ and $E_{g,\text{GaAs}}$ represent the band gap energies of the compounds InN and GaAs which were considered to be 1.95 and 3.4 eV, respectively, and b is the bowing parameter which was assumed to be 1.4. The effective masses^{13,14} were obtained through a linear extrapolation between the effective masses of InN and GaAs. The band offset ratio $\Delta E_C:\Delta E_V$ was considered to be 55:45.¹²

The 1-1 transition energy positions of the as grown and of the long annealed $\text{In}_x\text{Ga}_{1-x}\text{As}/\text{GaAs}$ and $\text{In}_x\text{Ga}_{1-x}\text{N}/\text{GaN}$ QDs of different shapes and dimensions were computed. The results obtained are shown in Figs. 2–6. Figure 2 depicts a schematic of the PL spectra for triangular and rectangular QWs corresponding to pyramidal, truncated pyramidal, and lens shaped $\text{In}_x\text{Ga}_{1-x}\text{As}/\text{GaAs}$ QDs computed in the same way as in our earlier report³ with initial indium concentration of 0.8. For a lens shaped dot having height (h)=10 nm and base (b)=30 nm, the PL peak energy corresponding to the peak PL intensity for the as grown

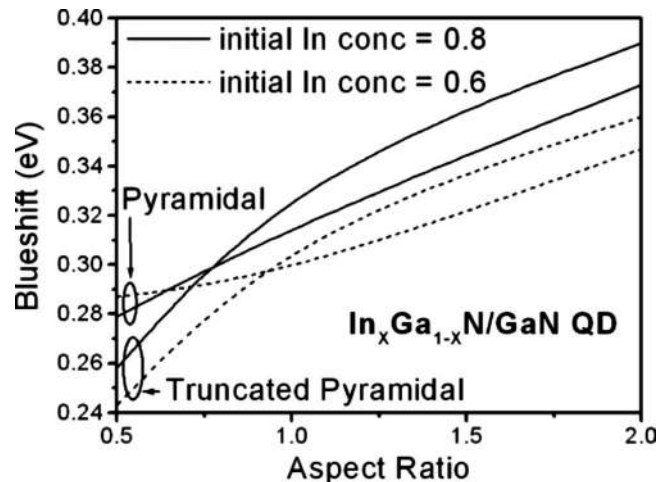


FIG. 5. Variation of the blueshift with the aspect ratio for pyramidal and truncated pyramidal $\text{In}_x\text{Ga}_{1-x}\text{N}/\text{GaN}$ QDs for two different initial indium concentrations 0.8 and 0.6.

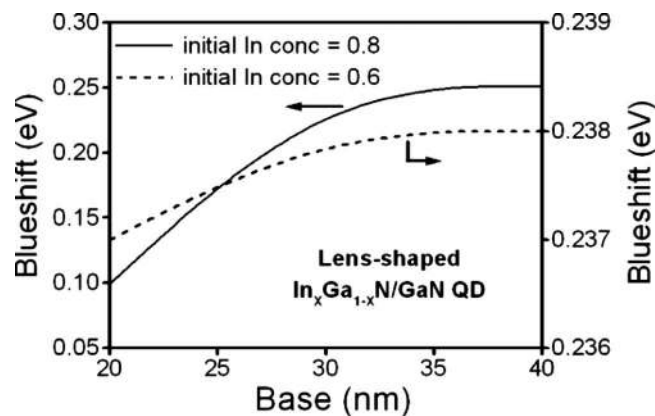


FIG. 6. Variation of the blueshift with the base for lens shaped $\text{In}_x\text{Ga}_{1-x}\text{N}/\text{GaN}$ dots for two different initial indium concentrations 0.8 and 0.6.

structure and of the long annealed $\text{In}_x\text{Ga}_{1-x}\text{As}/\text{GaAs}$ QD were found to be 1.263 and 1.396 eV, respectively, which gives a blueshift of 0.133 eV, as shown in Fig. 2. The blueshifts corresponding to pyramidal and truncated pyramidal structures were found to be 0.139 and 0.106 eV, respectively, which are pictorially represented in the same figure.

Figures 3 and 5 show the variation of the blueshift with the aspect ratio (height-to-base ratio) for pyramidal and truncated pyramidal $\text{In}_x\text{Ga}_{1-x}\text{As}/\text{GaAs}$ and $\text{In}_x\text{Ga}_{1-x}\text{N}/\text{GaN}$ QDs for two different initial indium concentrations 0.8 and 0.6. As the dimension of the QDs is typically 5–50 nm (Ref. 8) and in order to keep the complexity within presentable limits, we have varied the aspect ratio from 0.5 to 2.0. It could be inferred from Figs. 3 and 5 that the blueshift increases monotonically with increased dot dimension. Figures 4 and 6 represent the variation of the blueshift with base for lens shaped $\text{In}_x\text{Ga}_{1-x}\text{As}/\text{GaAs}$ and $\text{In}_x\text{Ga}_{1-x}\text{N}/\text{GaN}$ dots having height 10 nm. The blueshift tends to saturate at higher dot dimension. While calculating the PL peaks, the spreads in the PL spectra of long annealed pyramidal, truncated pyramidal, and lens shaped $\text{In}_x\text{Ga}_{1-x}\text{As}/\text{GaAs}$ dots, all having similar dimensions ($h=10$ nm and $b=20$ nm) with initial indium concentration of 0.8, were found to be 0.143, 0.111, and 0.053 eV. This suggests that the PL spectra of post-growth annealed lens shaped QDs are sharper than other dot structures considered in this work. To explain this we consider three different geometries of the annealed QD, pyramidal, truncated pyramidal, and lens shaped, having same aspect ratio as depicted in Fig. 7. a and b represent two vertical sections starting from the substrate end to the outer periphery in the growth direction. The QWs formed at section a corresponding to all types of geometry will have the same well width. Whereas, the QW formed at section b corresponding to lens shaped geometry will have the largest well width as compared to the pyramidal and truncated pyramidal struc-

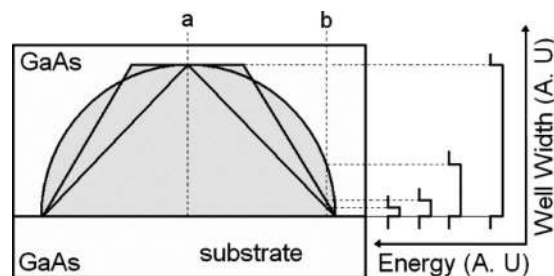


FIG. 7. Schematic illustration of three different geometries of the annealed QD, pyramidal, truncated pyramidal, and lens shaped, having same aspect ratio.

ture. The height of the QWs remains same for all geometries due to homogenization of indium and gallium in the annealed QDs. Thus the maximum PL energy corresponding to the QW of a lens shaped geometry for any section near the end periphery is less as compared to the pyramidal and truncated pyramidal structure. This makes the PL spectra of post-growth annealed lens shaped QDs sharper.

In summary, we have shown the dependence of the PL spectra of the as grown and long annealed $\text{In}_x\text{Ga}_{1-x}\text{As}/\text{GaAs}$ and $\text{In}_x\text{Ga}_{1-x}\text{N}/\text{GaN}$ QDs having pyramidal, truncated pyramidal, and lens shaped structures, which are of practical interest, through quantum mechanical model. The variation of the blueshift with the dot shape and dimension is presented. For pyramidal, truncated pyramidal dots, the blueshift increases monotonically with varying aspect ratio. In case of lens shaped dots, the blueshift increases initially and seems to saturate at larger dot dimensions. The PL spectra of long annealed lens shaped dot structures were found to be sharper than the other structures indicating an improved optical property desirable for optoelectronics application.

¹R. Leon, D. R. M. Williams, J. Krueger, E. R. Weber, and M. R. Melloch, *Phys. Rev. B* **56**, R4336 (1997).

²C. Lobo, R. Leon, S. Fafrad, and P. G. Piva, *Appl. Phys. Lett.* **72**, 2850 (1998).

³D. Biswas, S. Kumar, and T. Das, *J. Appl. Phys.* **101**, 026108 (2007).

⁴R. Leon, Y. Kim, C. Jagadish, M. Gal, J. Zou, and D. J. H. Cockayne, *Appl. Phys. Lett.* **69**, 1888 (1996).

⁵C.-C. Chuo, C.-M. Lee, T.-E. Nee, and J.-I. Chyi, *Appl. Phys. Lett.* **76**, 3902 (2000).

⁶Y.-S. Lin, K.-J. Ma, C. Hsu, Y.-Y. Chung, C.-W. Liu, S.-W. Feng, Y.-C. Cheng, C. C. Yang, and M. -H. Mao, *Appl. Phys. Lett.* **80**, 2571 (2002).

⁷Y.-S. Lin, K.-J. Ma, C.-C. Yang, and T. E. Weirich, *J. Mater. Sci.: Mater. Electron.* **14**, 49 (2003).

⁸O. Gunawan, H. S. Djite, and B. S. Ooi, *Phys. Rev. B* **71**, 205319 (2005).

⁹For example, see D. Bimberg, M. Grundmann, and N. N. Ledentsov, *Quantum Dot Heterostructures* (Wiley, Chichester, 1999).

¹⁰J.-W. Luo, S.-S. Li, J.-B. Xia, and L.-W. Wang, *Phys. Rev. B* **71**, 245315 (2005).

¹¹H. Heidemeyer, U. Denker, C. Muller, and O. G. Schmidt, *Phys. Rev. Lett.* **91**, 196103 (2003).

¹²D. Biswas, S. Kumar, and T. Das, *Thin Solid Films* **515**, 4488 (2007).

¹³J.-J. Shi and Z.-Z. Gan, *J. Appl. Phys.* **94**, 407 (2003).

¹⁴C.-C. Chen, H.-W. Chuang, G.-C. Chi, C.-C. Chuo, and J.-I. Chyi, *Appl. Phys. Lett.* **77**, 3758 (2000).